

Cite this: *Chem. Sci.*, 2024, 15, 13032

All publication charges for this article have been paid for by the Royal Society of Chemistry

Received 25th June 2024  
Accepted 12th July 2024

DOI: 10.1039/d4sc04190a

rsc.li/chemical-science

# Metal $\pi$ -Lewis base activation in palladium(0)-catalyzed *trans*-alkylative cyclization of alkynals†

Lei Zhu,<sup>†ab</sup> Bo Zhao,<sup>†a</sup> Ke Xie,<sup>c</sup> Wu-Tao Gui,<sup>c</sup> Sheng-Li Niu,<sup>a</sup> Peng-Fei Zheng,<sup>a</sup> Ying-chun Chen,<sup>†ac</sup> Xiao-Wei Qi<sup>\*b</sup> and Qin Ouyang<sup>†\*a</sup>

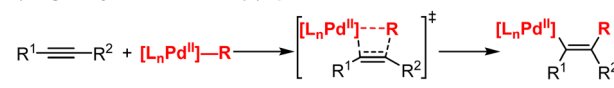
The Pd(0)-mediated umpolung reaction of an alkyne to achieve *trans*-difunctionalization is a potential synthetic methodology, but its insightful activation mechanism of Pd(0)–alkyne interaction has yet to be established. Here, a Pd(0)– $\pi$ -Lewis base activation mode is proposed and investigated by combining theoretical and experimental studies. In this activation mode, the Pd(0) coordinates to the alkyne group and enhances its nucleophilicity through  $\pi$ -back-donation, facilitating the nucleophilic attack on the aldehyde to generate a *trans*-Pd(II)–vinyl complex. Ligand-effect studies reveal that the more electron-donating one would accelerate the reaction, and the cyclization of the challenging flexible C- or O-tethered substrates has been realized. The origin of regioselectivities is also explicated by the newly proposed metal  $\pi$ -Lewis base activation mode.

## Introduction

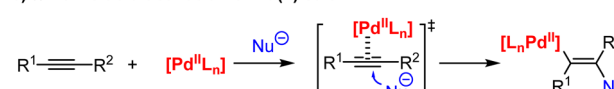
Transition metal-catalyzed transformations of alkynes have been widely used in the preparation of organic intermediates, bioactive molecules, and optical materials, owing to the unique nucleophilic and electrophilic potentials of the C–C triple bond.<sup>1</sup> Among them, palladium catalysis always occupies a leading position and has been applied to the construction of various C–X bonds.<sup>2</sup> In the current stage of this art, the activation of alkynes by palladium occurs *via* two major modes: (1) migratory insertion of organopalladium reagents formed *via* oxidative addition, C–H bond activation or transmetalation to the alkynes to give vinyl–Pd species (Scheme 1a);<sup>1e,3</sup> (2) metal  $\pi$ -Lewis acid activation, in which  $\pi$ -coordination of an electrophilic Pd(II) complex removes electron density from the alkynes and renders an outer-sphere nucleophilic attack (Scheme 1b).<sup>4</sup> In general, alkynes act as electrophilic partners in both modes, which might significantly restrict the potential of Pd-catalyzed transformations. In fact, the Pd-mediated nucleophilic addition reaction of alkynes has been significantly underdeveloped.

Tsukamoto and co-workers uncovered an intriguing Pd(0)-catalyzed intramolecular alkylative cyclization of alkynal

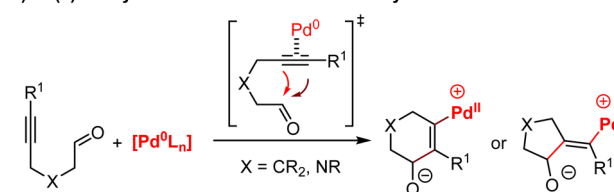
### a) Migratory insertion of Pd(II) species



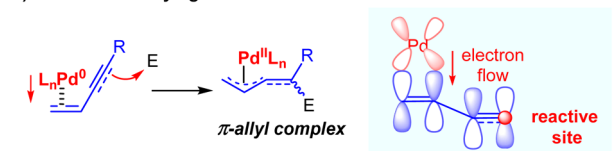
### b) $\pi$ -Lewis acid activation of Pd(II) salt



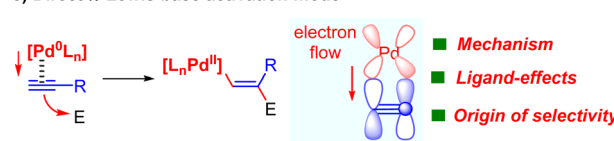
### c) Pd(0)-catalyzed *anti*-Wacker reaction of alkynals



### d) Established vinylogous $\pi$ -Lewis base activation



### e) Direct $\pi$ -Lewis base activation mode



**Scheme 1** Diverse activation modes for Pd-catalyzed transformations involving alkynes. (a) Migratory insertion; (b)  $\pi$ -Lewis acid activation; (c) Pd(0)-catalyzed intramolecular alkylative cyclization; (d) vinylogous  $\pi$ -Lewis base activation; (e) direct  $\pi$ -Lewis base activation.

<sup>a</sup>College of Pharmacy, Third Military Medical University, Shapingba, Chongqing 400038, China. E-mail: ouyangq@tmmu.edu.cn

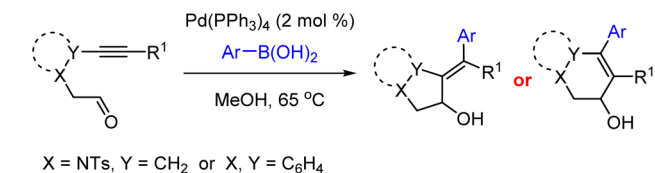
<sup>b</sup>Breast and Thyroid Surgery, Southwest Hospital, Third Military Medical University, Shapingba, Chongqing 400038, China. E-mail: qwx9908@foxmail.com

<sup>c</sup>Key Laboratory of Drug-Targeting and Drug Delivery System of the Ministry of Education and Sichuan Research Center for Drug Precision Industrial Technology, West China School of Pharmacy, Sichuan University, Chengdu 610041, China

† Electronic supplementary information (ESI) available. See DOI: <https://doi.org/10.1039/d4sc04190a>

‡ These authors contributed equally.





Scheme 2 Pd(0)-catalyzed alkyne functionalization with electrophiles.

substrates followed by a cascade Suzuki reaction with organo-boronic reagents.<sup>5</sup> Unexpectedly, this transformation proceeded *trans*-selectively against the Ni or Rh-mediated *cis*-oxidative cyclometallation process,<sup>6</sup> and a formal anti-Wacker-type activation mode, in which the Pd(0) catalyst coordinates with the alkyne guiding the nucleophilic attack on the carbonyl functionality, was proposed (Scheme 1c).<sup>7</sup> However, the catalytic mechanism, especially the intrinsic Pd(0)-alkyne interaction in

this activation mode remains unclear. Due to the lack of theoretical awareness of such an activation mode, the development of Pd(0)-mediated nucleophilic reactions of alkynes was yet at a standstill in recent years.

In a Chatt–Dewar–Duncanson coordination mode, besides the Pd acting as a  $\pi$ -Lewis acid by accepting  $\pi$ -electrons of alkynes, the empty antibonding molecular orbital of the alkyne ( $\pi^*$ ) is able to accept electrons from the d-orbitals of Pd *via*  $\pi$ -back-donation.<sup>8</sup> Thus it can provide a possible catalytic mode *via*  $\pi$ -Lewis base activation.<sup>9</sup> Our recent studies indicate that Pd(0) can activate 1,3-dienes<sup>10</sup> and 1,3-enynes<sup>11</sup> to react with electrophilic partners *via*  $\eta^2$ -coordination in a vinylogous manner, in which the generation of  $\pi$ -allylpalladium complexes supplies the essential driving force (Scheme 1d). These emphasize the potential of Pd(0) as a  $\pi$ -Lewis base catalyst to directly activate alkynes. Consequently, we speculated that a metal  $\pi$ -Lewis base activation mode would be reasonable for Pd(0)-catalyzed alkylative transformation of alkynals. The

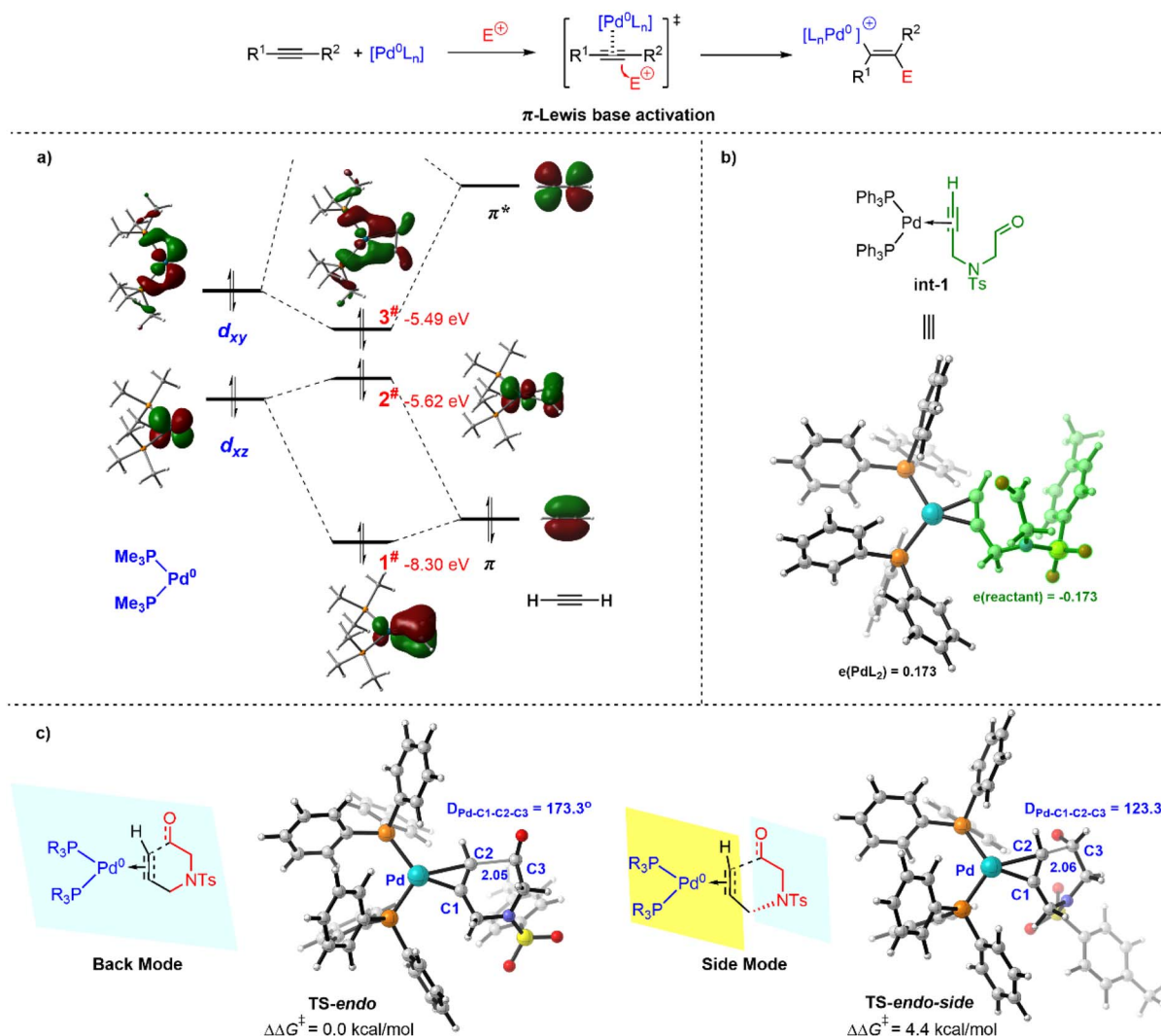


Fig. 1 Pd(0)- $\pi$ -Lewis base activation of alkynes. (a) Molecular orbital analysis for Pd(0) and alkyne. (Me<sub>3</sub>)<sub>2</sub>Pd(0) and acetylene were employed as a simplified model. (b) Mulliken charge distribution of  $\eta^2$ -coordinated Pd(0)-alkynal complex. (c) Comparison of back and side modes for  $\pi$ -Lewis base activation.



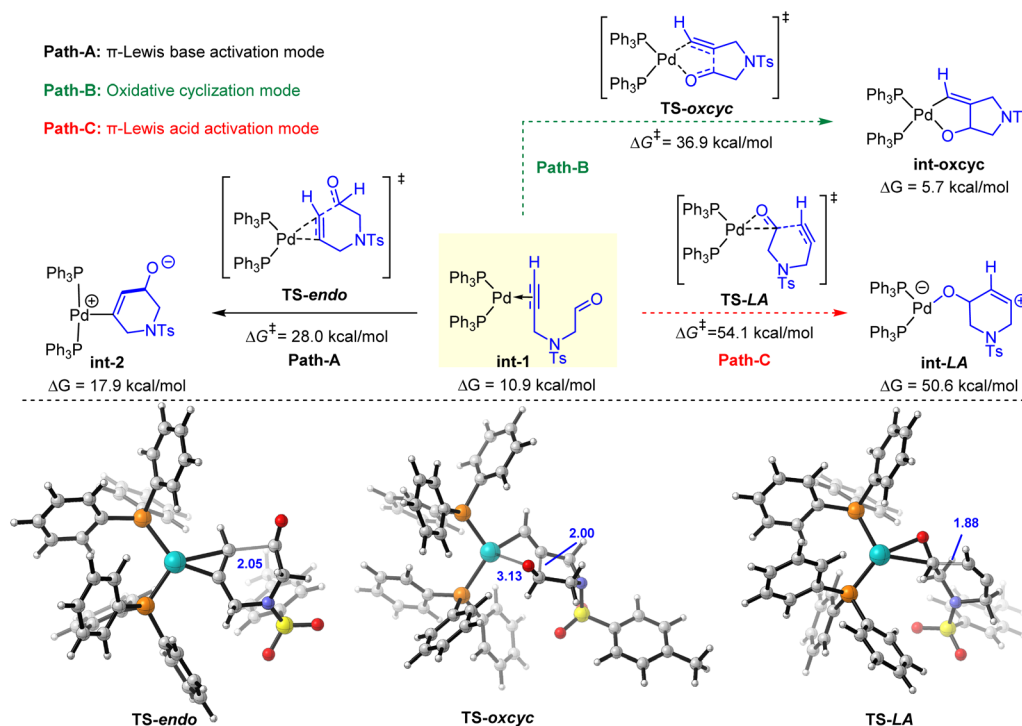


Fig. 2 Comparison of the  $\pi$ -Lewis base activation, oxidative cyclization, and  $\pi$ -Lewis acid activation modes.  $\Delta G$  in this figure is in kcal mol<sup>-1</sup> with respect to the Pd(PPh<sub>3</sub>)<sub>4</sub> and reactant alkyne **1a**.

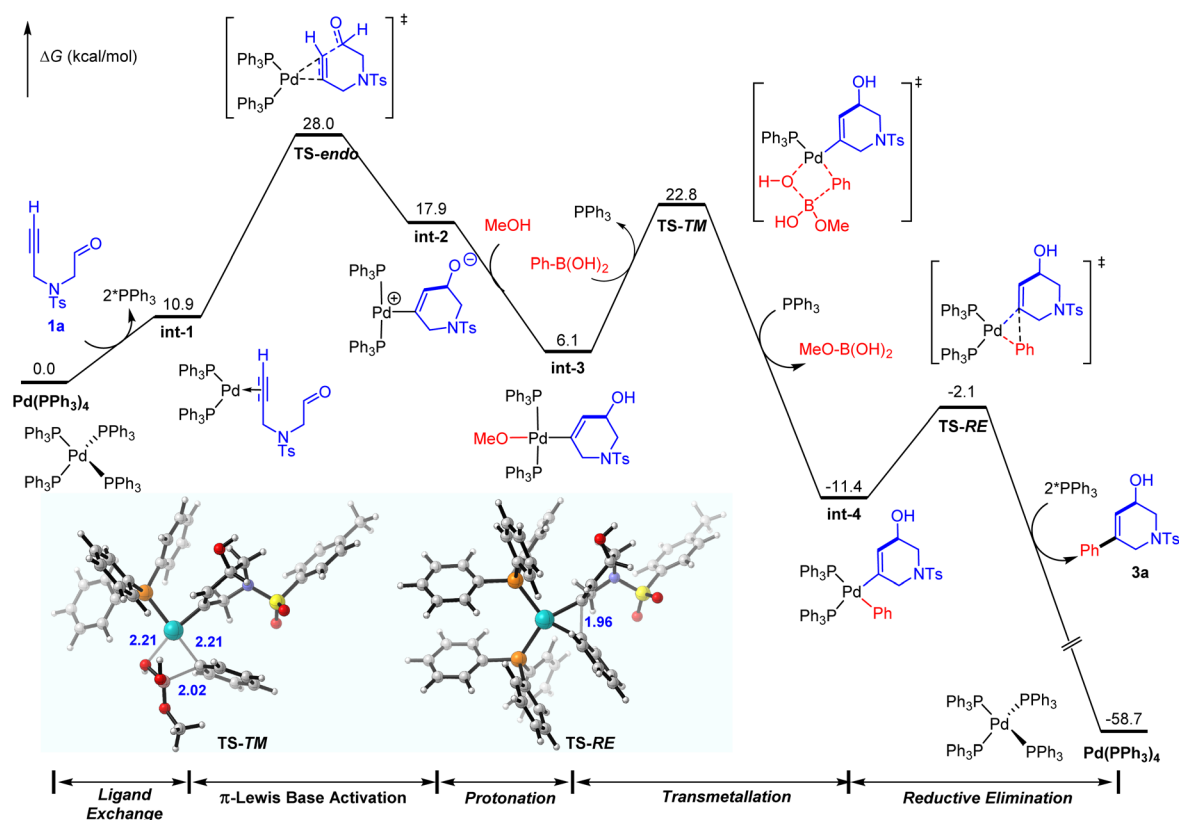


Fig. 3 Whole free energy profile for the Pd(0)-catalyzed *trans*-alkylative cyclization of the alkyne.



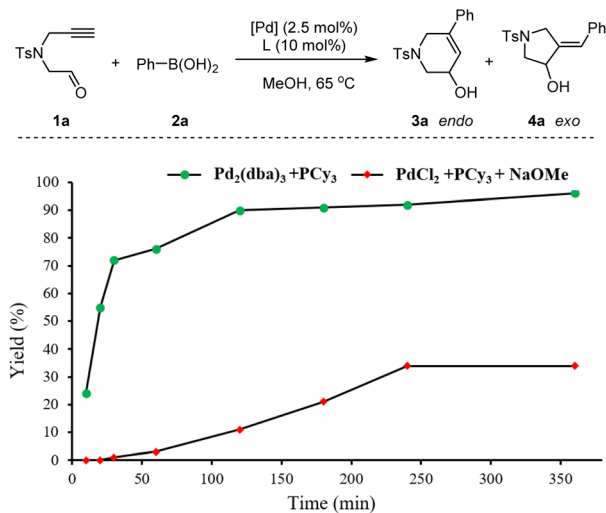


Fig. 4 Kinetic studies. The yield indicates the total yield of **3a** and **4a**.

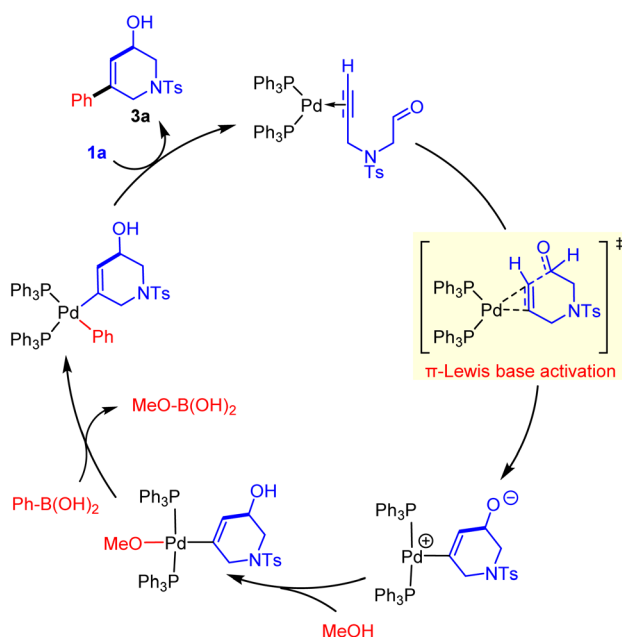


Fig. 5 Proposed catalytic cycle.

electron flowing to the alkyne from the electron-rich Pd(0) center through  $\pi$ -back-donation would enhance the nucleophilic reactivity of the  $\eta^2$ -coordinated Pd(0)-alkyne complex, which would allow a Friedel-Crafts type reaction with electrophilic partners to generate a vinyl-Pd(II) complex (Scheme 1e).

Herein, we carried out a mechanistic study on Pd(0)-catalyzed alkyne transformation, using Tsukamoto's report as a model reaction to elucidate our newly proposed metal  $\pi$ -Lewis base activation mode (Scheme 2).<sup>5a</sup> We performed a combined theoretical and experimental investigation on the activation mechanism, ligand effects, and origin of selectivity. Importantly, inspired by the theoretical understandings, this Pd(0)-catalyzed transformation was consequently extended to adapt the more flexible C-tethered or O-tethered alkynal substrates.

## Computational methods

In this work, all of the density functional theory (DFT) calculations were performed using Gaussian 09<sup>12</sup> software packages. The B3LYP<sup>13</sup> function together with the Def2-SVP basis set was used for the geometry optimization and frequency analysis. Vibrational frequency calculations were performed for all the stationary points to confirm if each optimized structure is a local minimum or a transition state structure, as well as derive the thermochemical corrections for the enthalpies and free energies. The intrinsic reaction coordinate (IRC) path was performed to check the energy profiles connecting each transition state to two associated minima of the proposed intermediates. After optimization, the M06<sup>14</sup> function with the Def2-TZVP basis set was used to calculate the single-point energies to give more accurate energy information. The integration grids defined by the Int=Ultrafine keyword were used for all calculations. Besides, the solvent effect was considered by single-point calculations at the gas-phase stationary points with the SMD solvation model.<sup>15</sup> When obtaining the relative Gibbs energy at 298 K, a correction of  $-2.6$  (or  $2.6$ ) kcal mol<sup>-1</sup> was performed for the transformation involving two molecules into one molecule (or one molecule into two molecules), to reduce the overestimation of entropy contribution.<sup>16</sup> Optimized structures are illustrated by using CYLview.<sup>17</sup>

## Results and discussion

### Explication of Pd(0)- $\pi$ -Lewis base activation mode

At the outset of this study, we devoted ourselves to investigating the nature of Pd(0)-mediated  $\pi$ -Lewis base activation of alkynes. As depicted in our aforementioned metal  $\pi$ -Lewis base activation mode, when an alkyne coordinates to the Pd(0) center, the electron flows from the electron-rich Pd(0) center to the alkyne through back donation. It would result in the increase of the HOMO-energy of the  $\eta^2$ -coordinated Pd(0)-alkyne complex as well as the enhancement of electron density for the alkyne moiety. To validate this, we conducted the molecular orbitals (MO) and natural population analysis (NPA) for the Pd(0)-alkyne complex.

As shown in Fig. 1a, the complex of acetylene and (PMe<sub>3</sub>)<sub>2</sub>Pd(0) was employed as a model for the molecular orbital interaction analysis. The d-orbitals are considered to have  $\pi$ -symmetry, which could interact with  $\pi$  and  $\pi^*$  of the alkyne. For the d/ $\pi$  interaction, the bonding combination of  $d_{xz}$  and  $\pi$  gives rise to 1<sup>#</sup> orbital, and the antibonding combination results in 2<sup>#</sup> orbital. Meanwhile, the 3<sup>#</sup> orbital is derived by the bonding combination of  $d_{xy}$  and  $\pi^*$  echoing the d/ $\pi^*$  interaction, which indicates a significant back donation. The 3<sup>#</sup> and 2<sup>#</sup> orbitals are the HOMO and HOMO-1 for the (Me<sub>3</sub>)<sub>2</sub>Pd(0)-acetylene complex, which is much higher than the HOMO of acetylene ( $-8.06$  eV). It suggests that the nucleophilicity of the (Me<sub>3</sub>)<sub>2</sub>Pd(0)-acetylene complex is essentially enhanced and qualified for a Friedel-Crafts type process, due to the activation by the Pd(0) catalyst. Moreover, the computed Mulliken charge of the PdL<sub>2</sub> fragment in the (Ph<sub>3</sub>)<sub>2</sub>Pd(0)-alkynal complex **int-1** is  $+0.173$ , indicating a considerable amount of charge transfer



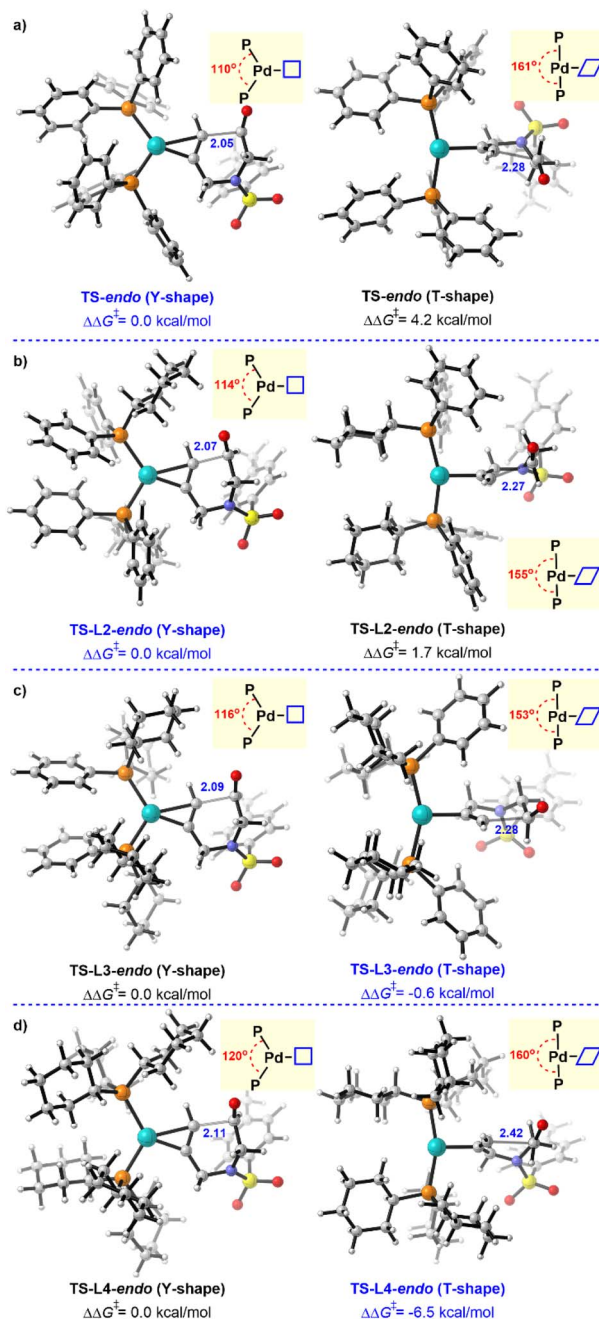


Fig. 6 Ligand effects for Pd(0)- $\pi$ -Lewis base activation of alkynes.

from  $\text{PdL}_2$  to alkyne **1a** (Fig. 1b).<sup>18</sup> It further reveals the increase of electron density for the alkyne moiety in the  $\pi$ -Lewis base activation mode.

The nodal planes of orbital  $2^\#$  and  $3^\#$  are perpendicular and their orbital energy levels are close, so both of them may exhibit related reactivity. It means the electrophilic partners could react in the back (referring to  $3^\#$ ) or side direction (referring to  $2^\#$ ) of the alkyne. Therefore, we then evaluated the reactivity of the back and side modes for  $\pi$ -Lewis base activation. As depicted in Fig. 1c, the dihedral angle  $\text{D}_{\text{Pd-C1-C2-C3}}$  is  $173.3^\circ$  in the transition state **TS-endo**, and the corresponding dihedral angle is  $123.3^\circ$  in **TS-endo-side**, relating to the back and side modes, respectively.

Calculated results show that the relative free energy of **TS-endo** is  $4.4 \text{ kcal mol}^{-1}$  lower than that of **TS-endo-side**, which is correlated with the molecular orbital energy of  $2^\#$  and  $3^\#$ . It suggests that the back mode is more favorable in this Pd(0)-catalyzed  $\pi$ -Lewis base activation of alkyne **1a**.

### Comparison of different activation modes

With the activation mode constructed, we then evaluated the reactivity difference for the  $\pi$ -Lewis base activation and others. As shown in Fig. 2, three activation modes including  $\pi$ -Lewis base activation (Path-A), oxidative cyclization (Path-B), and  $\pi$ -Lewis acid activation (Path-C) were taken into consideration. The active  $(\text{Ph}_3)_2\text{Pd}(0)$ -alkyne complex **int-1** could be generated after the ligand exchange between  $\text{Pd}(\text{PPh}_3)_4$  and reactant alkyne **1a**, which is endergonic by  $10.9 \text{ kcal mol}^{-1}$ . Starting from **int-1**, the  $\pi$ -Lewis base activation (Path-A) proceeds via **TS-endo** with a moderate activation free energy of  $28.0 \text{ kcal mol}^{-1}$ . As a result, the zwitterionic *trans*-Pd(II)-vinyl complex **int-2** was formed, which allows a follow-up Suzuki reaction to access the *trans*-difunctionalized product. Meanwhile, MeOH and arylboronic acid are considered to stabilize the alkoxide in the  $\pi$ -Lewis base activation mode but these processes possess high energy barriers (Fig. S2†). The vinyl five-membered palladacycle complex **int-oxcyc** could be generated through oxidative cyclization (Path-B).<sup>19</sup> Although this process is less endothermic than Path-A, the activation free energy is  $36.9 \text{ kcal mol}^{-1}$  (referring to **TS-oxcyc**), indicating it is kinetically unfavorable. This is consistent with the observation of the absence of *cis*-difunctionalized products. In addition, the Pd(0) catalyst could be considered as a Lewis acid to activate the aldehyde moiety (Path-C). However, the activation free energy of this pathway is extremely high, about  $54.1 \text{ kcal mol}^{-1}$  (referring to **TS-LA**), which reveals the insufficient Lewis acidity of the Pd(0) complex. Therefore, these results suggest that this Pd(0)-catalyzed *trans*-difunctionalization of alkyne **1a** would preferentially undergo the  $\pi$ -Lewis base activation pathway.

### Catalytic cycle

As shown in Fig. 3, starting from the zwitterionic Pd(II)-vinyl complex **int-2**, the protonation by methanol affords the neutral *trans*-Pd(II)-vinyl-OMe complex **int-3**, and the generated counter ion  $\text{MeO}^-$  could be considered as an activator of phenylboronic acid to realize the following Suzuki reaction.<sup>20</sup> It proves that MeOH was a critical solvent in the experiment.<sup>5a</sup> Subsequent transmetalation proceeds via the four-centered cyclic transition state **TS-TM** with an energy barrier of  $16.7 \text{ kcal mol}^{-1}$ , in which one of the  $\text{PPh}_3$  was dissociated to afford unsaturation.<sup>21</sup> This transmetalation process is driven by the formation of a stable B-O bond in  $\text{MeO-B}(\text{OH})_2$ , and gives the Pd(II)-vinyl-phenyl complex **int-4** irreversibly. Then the C-C reductive elimination occurs rapidly to release the final *trans*-difunctionalized product **3a**, and the active  $(\text{Ph}_3)_2\text{Pd}(0)$ -alkyne complex **int-1** is also regenerated.

Moreover, to exclude the possibility of the Pd(II)-catalyzed mechanism involving sequential transmetalation, alkyne 1,2-carbopalladation, *Z/E*-isomerization, intramolecular aldehyde



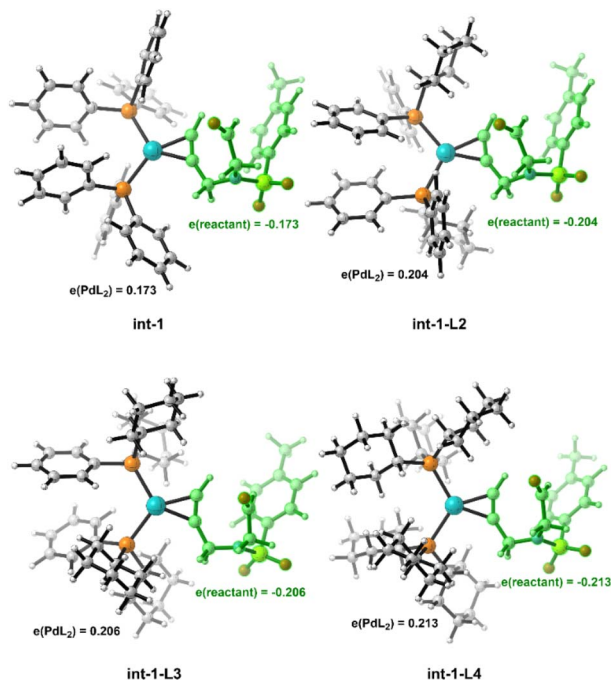


Fig. 7 Mulliken charge distribution of the  $\eta^2$ -coordinated Pd(0)-alkynal complex with PPh<sub>3</sub> (L1), PPh<sub>2</sub>Cy (L2), PPhCy<sub>2</sub> (L3), and PCy<sub>3</sub> (L4).

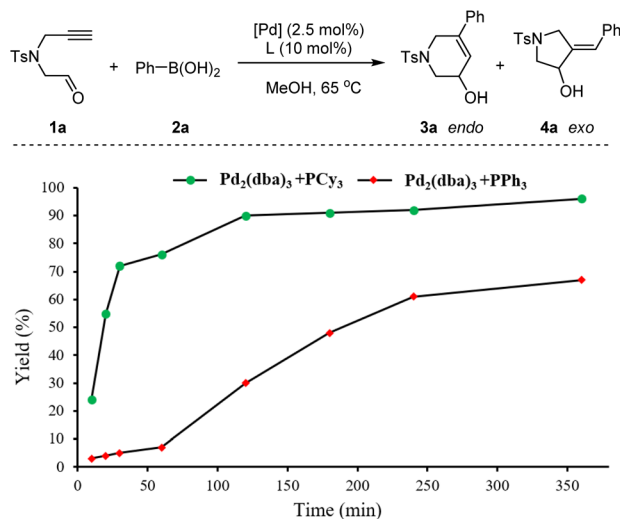


Fig. 8 Kinetic studies. The yield indicates the total yield of **3a** and **4a**.

1,2-addition, and protonation, further calculations and control experiments were also conducted. The calculated results indicate that *Z/E*-isomerization is the rate-determining step of the Pd(II)-mediated reaction pathway. Its activation energy is 28.6 kcal mol<sup>-1</sup> (**TS-3** in Fig. S4†), which is close to the activation energy of the Pd(0)-mediated reaction pathway in Fig. 3 (28.0 kcal mol<sup>-1</sup>, *via TS-endo*). However, the reduction of Pd(II) with the assistance of phenylboronic acid to generate a Pd(0) catalyst is more favorable than the Pd(II)-mediated reaction pathway (Fig. S4†). Moreover, the corresponding biphenyl by-product

was detected in the further control experiment, which corroborates the calculated results (Fig. S5†). Further kinetic studies of the comparison of Pd(0) and Pd(II) catalysts show a low reaction rate as well as an obvious induction period in the Pd(II)-catalyzed system (Fig. 4). These results validate our mechanistic speculation of the reduction of Pd(II) with the assistance of phenylboronic acid to generate the active Pd(0) catalyst *in situ*. (See the ESI† for more details.)

Thus far, the whole catalytic cycle of the Pd(0)-catalyzed *trans*-alkylative cyclization of alkynals was constructed, which undergoes a sequential  $\pi$ -Lewis base activation, protonation, transmetalation, and reductive elimination (Fig. 5). Among them, the  $\pi$ -Lewis base activation step is identified as the rate-determining step.

### Ligand effects

Ligands were recognized to regulate the reactivity and selectivity in this catalytic system. We then turned to explore the ligand effects for this Pd(0)-catalyzed  $\pi$ -Lewis base activation. As shown in Fig. 6a, the transition state **TS-endo** (marked as a Y-Shape) presents a trigonal planar geometry, in which the bite angle  $\angle_{P-Pd-P}$  is 110°. The reacting alkyne is parallel to the P-Pd-P plane. Meanwhile, another transition state was also found [**TS-endo** (T-Shape)], in which the conformation of the transition state rearranged to a T-shape.<sup>36,22</sup> The relative free energy of **TS-endo** (T-Shape) is 4.2 kcal mol<sup>-1</sup> higher than that of **TS-endo** (Y-Shape). This energy discrepancy could be attributed to the reduced orbital overlap between Pd and reactant, owing to the reacting alkyne being perpendicular to the P-Pd-P plane in **TS-endo** (T-shape) (Fig. S7†). In a sense, the perpendicular conformation would release the steric hindrance to the reactant-ligand and ligand-ligand. We thus speculated that when bulky ligands were employed, the T-shape conformation could be preferred. To clarify this, a series of ligands PPh<sub>2</sub>Cy (**L2**), PPhCy<sub>2</sub> (**L3**), and PCy<sub>3</sub> (**L4**), with steric hindrance increased, were then evaluated. Expectedly, the corresponding energy discrepancy was reduced when one cyclohexyl was introduced (Fig. 6b), and it was inverted when two-cyclohexyl substituted **L3** was used (Fig. 6c). Furthermore, the T-shape conformation (**TS-L4-endo** (T-Shape)) becomes plenary preferred in the PCy<sub>3</sub> (**L4**) involved case (Fig. 6d).

These results suggest that the Pd(0)-catalyzed  $\pi$ -Lewis base activation could undergo different transition state conformations for PPh<sub>3</sub> (**L1**) and PCy<sub>3</sub> (**L4**), which would result in different reactivities.

The crucial feature of the Pd(0)- $\pi$ -Lewis base activation mode is the electron donation of Pd(0), so the electron effect of the ligand should also matter. Calculated results show that the amounts of charge transfer from PdL<sub>2</sub> to alkynal **1a** are gradually increased along with the enhanced electron-donating ability of ligands (**L1**  $\rightarrow$  **L4**) (Fig. 7). Moreover, the free energy barrier of the **L4**-involved case is 8.7 kcal mol<sup>-1</sup> lower than that of **L1** (Fig. S8†), correlating with the electron-donating effects. It indicates that ligands with greater electron-donating ability would accelerate the Pd(0)-catalyzed  $\pi$ -Lewis base activation reaction. To verify this concept, we then conducted the kinetic

Table 1 Reaction of C- or O-tethered substrates<sup>a</sup>

Entry	1	L	Temp. (°C)	Yield <sup>b</sup> (%)	endo/exo
1	1b	L1(PPh <sub>3</sub> )	60–100	N.D.	—
2	1b	L4(PCy <sub>3</sub> )	80	3b, 64	>19 : 1
3	1b	L4(PCy <sub>3</sub> )	100	3b, 97 (85) <sup>c</sup>	>19 : 1
4	1c	L4(PCy <sub>3</sub> )	100	3c, 43	>19 : 1

<sup>a</sup> Conditions: **1** (0.2 mmol), **2** (0.3 mmol), Pd<sub>2</sub>(dba)<sub>3</sub> (5 mol%), **L** (30 mol%), MeOH (0.1 M), for 24 h under a nitrogen atmosphere. <sup>b</sup> Determined by <sup>1</sup>H NMR analysis. <sup>c</sup> Isolated yield. The Ar of Ar-B(OH)<sub>2</sub> represents *p*-tolyl.

experiments. As shown in Fig. 8, the reaction could achieve over 70% yield within 30 minutes in the presence of PCy<sub>3</sub> (**L4**), and it was almost complete within 2 hours.<sup>23</sup> In contrast, the corresponding reaction with PPh<sub>3</sub> (**L1**) takes 6 hours to complete, which demonstrates the significant acceleration of the electron-donating ligand PCy<sub>3</sub> (**L4**).

Based on the above results, we speculate if the more electron-donating ligand PCy<sub>3</sub> (**L4**) could realize the Pd(0)-catalyzed  $\pi$ -Lewis base activation reaction of challenging C- or O-tethered 1,5-alkynals. We initiated the reaction between O-tethered 1,5-alkynal **1b** and *p*-tolylboronic acid **2b** under the catalysis of Pd<sub>2</sub>(dba)<sub>3</sub> and PPh<sub>3</sub> (**L1**). Unsurprisingly, there are no desired products **3b** or **4b** detected from 60 to 100 °C (Table 1, entry 1), which distinguishes the inertness of the O-tethered substrate **1b**. However, when PCy<sub>3</sub> (**L4**) was used, **3b** was obtained in a moderate yield with over 19 : 1 regioselectivity at 80 °C. The yield could be improved to 97% (85% isolated yield) at 100 °C. Moreover, the reaction of C-tethered substrate **1c** could also give an acceptable yield for product **3c**. These results further

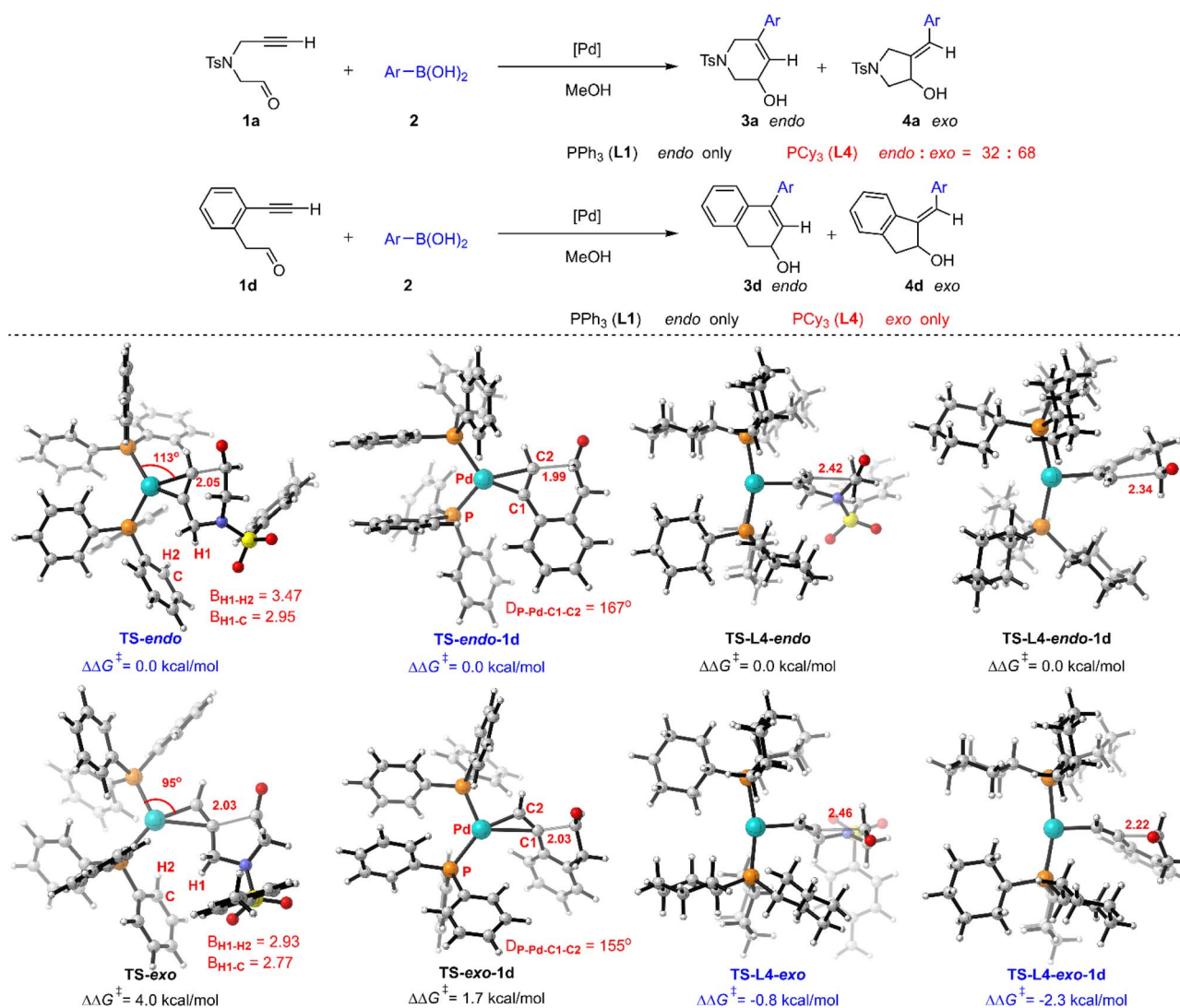


Fig. 9 Origin of regioselectivities. The Ar of Ar-B(OH)<sub>2</sub> represents *p*-tolyl.



emphasize the crucial role of electron-donating effects in the Pd(0)- $\pi$ -Lewis base activation of alkynes.

### Origin of regioselectivity

The reaction only gave *endo*-products no matter whether alkyl (**1a**) or aryl (**1d**) substituted reactants were used in the presence of PPh<sub>3</sub> (**L1**), while the corresponding regioselectivities were changed when PCy<sub>3</sub> (**L4**) was employed (Fig. 9).<sup>5a</sup> We then turned to reveal the origin of regioselectivity for this Pd(0)- $\pi$ -Lewis base activation, based on the understanding of ligand effects. The calculated results show that the relative free energy of **TS-endo** is 4.0 kcal mol<sup>-1</sup> lower than that of **TS-exo**, indicating the priority of *endo*-selectivity, which corroborates with the experimental observation. The steric hindrance between the proximal methylene and ligand makes **TS-exo** present a heterogenic trigonal planar geometry (referring to the change of the P-Pd-C angle from 115° (**TS-endo**) to 95° (**TS-exo**)), which results in its high energy. For aryl-tethered **1d**, the electron-withdrawing aryl substituent within the tether may enhance the reactivity of the internal position of the alkyne to access the *exo*-product **4d**. But this steric hindrance caused by the aryl group makes the reacting alkyne deviate from the P-Pd-P plane in **TS-exo-1d** (the corresponding dihedral angle D<sub>P-Pd-C1-C2</sub> is 155°), which results in its relative free energy still being 1.7 kcal mol<sup>-1</sup> higher than that of **TS-endo-1d**. Thus, the *endo*-product **3d** was majorly obtained in the presence of PPh<sub>3</sub> (**L1**). These results suggest that the steric effect dominates the regioselectivity in the PPh<sub>3</sub> (**L1**) involved case.

Moreover, the T-shape conformation is preferred in the PCy<sub>3</sub> (**L4**) involved case, in which the steric hindrance is partially released. Thus, the relative free energy of **TS-L4-exo** is 0.8 kcal mol<sup>-1</sup> lower than that of **TS-L4-endo** due to the weak electron-donating effects of the alkyl moiety at **1a**, which is consistent with the observation of the mixture (*endo/exo* = 32 : 68) in the experiment. Meanwhile, the electron-withdrawing aryl group at **1d** guides the nucleophilic attack, in which the relative free energy of **TS-L4-exo-1d** is 2.3 kcal mol<sup>-1</sup> lower than that of **TS-L4-endo-1d**, leading to the *exo*-selectivity. Furthermore, large substituents at the terminal position of NT-tethered reactants **1e** and **1f** lead to *endo*-selectivity in the presence of **L4**, and electron-withdrawing aryl substituent **1g** is more *endo*-selective (Fig. S9†). These results indicate that the regioselectivity depends on both steric and electronic effects in the PCy<sub>3</sub> (**L4**) involved case.

## Conclusions

In summary, the metal  $\pi$ -Lewis base activation mode for the Pd(0)-catalyzed *trans*-alkylative cyclization of alkynals has been disclosed by a combined theoretical and experimental study. In this activation mode, the electrons flow to the alkyne from the electron-rich Pd(0) center through back-donation to enhance the nucleophilic reactivity of the alkyne moiety. Thus the Pd(0)-coordinated alkyne could proceed with a nucleophilic addition to the aldehyde generating the *trans*-Pd(II)-vinyl complex. The computational results show that this metal  $\pi$ -Lewis base

activation mode is more favorable than the oxidative cyclization and  $\pi$ -Lewis acid activation. Ligand effect investigations indicate that the more electron-donating ligand would accelerate this reaction. As a result, the reaction for the challenging flexible C- or O-tethered substrates has been realized by using PCy<sub>3</sub>. The origin of regioselectivities is also explicated by the newly proposed metal  $\pi$ -Lewis base activation mode. Our studies provide a comprehensive mechanistic understanding of the Pd(0)-mediated umpolung reaction of alkynes, which could be notably extended to other related systems. We anticipate that it will provide a practical theoretical guide for further experimental development of Pd(0)-catalyzed transformations of alkynes.

## Data availability

All experimental procedures, details of the calculations, and additional data can be found in the ESI†.

## Author contributions

The manuscript was written through the contributions of all authors. All authors have approved the final version of the manuscript.

## Conflicts of interest

The authors declare no competing financial interest.

## Acknowledgements

We gratefully acknowledge the National Key R&D program of China (No. 2022YFC2502501), the National Natural Science Foundation of China (No. 22001264 and 22201302), and the Outstanding Youth Fund of Chongqing (2023NSCQ-JQX0081) for financial support.

## Notes and references

- (a) J. Corpas, P. Mauleón, R. G. Arrayás and J. C. Carretero, *ACS Catal.*, 2021, **11**, 7513–7551; (b) M. M. Haley, *Angew. Chem., Int. Ed.*, 2015, **54**, 8332; (c) A. L. Shi Shun and R. R. Tykwinski, *Angew. Chem., Int. Ed.*, 2006, **45**, 1034–1057; (d) T. T. Talele, *J. Med. Chem.*, 2020, **63**, 5625–5663; (e) Y. Yamamoto, *Chem. Soc. Rev.*, 2014, **43**, 1575–1600.
- (a) R. Chinchilla and C. Najera, *Chem. Rev.*, 2014, **114**, 1783–1826; (b) X. Huang, S. Liao, L. Xin, F. Zhang and Y. Yu, *Synthesis*, 2020, **53**, 238–254; (c) J. Li, D. He, Z. Lin, W. Wu and H. Jiang, *Org. Chem. Front.*, 2021, **8**, 3502–3524; (d) W. Wu and H. Jiang, *Acc. Chem. Res.*, 2012, **45**, 1736–1748.
- (a) V. P. Boyarskiy, D. S. Ryabukhin, N. A. Bokach and A. V. Vasilyev, *Chem. Rev.*, 2016, **116**, 5894–5986; (b) J. Escorihuela, A. Lledos and G. Ujaque, *Chem. Rev.*, 2023, **123**, 9139–9203; (c) L. Xue and Z. Lin, *Chem. Soc. Rev.*, 2010, **39**, 1692–1705.



- 4 (a) P. Davies and H. Adcock, *Synthesis*, 2012, **44**, 3401–3420; (b) G. Zeni and R. C. Larock, *Chem. Rev.*, 2004, **104**, 2285–2309.
- 5 (a) H. Tsukamoto, T. Ueno and Y. Kondo, *J. Am. Chem. Soc.*, 2006, **128**, 1406–1407; (b) H. Tsukamoto and Y. Kondo, *Angew. Chem., Int. Ed.*, 2008, **47**, 4851–4854; (c) H. Tsukamoto, K. Ito, T. Ueno, M. Shiraishi, Y. Kondo and T. Doi, *Chem.–Eur. J.*, 2023, **29**, e202203068.
- 6 (a) E. A. Standley, S. Z. Tasker, K. L. Jensen and T. F. Jamison, *Acc. Chem. Res.*, 2015, **48**, 1503–1514; (b) Y. Hoshimoto, M. Ohashi and S. Ogoshi, *Acc. Chem. Res.*, 2015, **48**, 1746–1755; (c) V. Piccialli, *Synthesis*, 2007, **2007**, 2585–2607; (d) R. Shintani, K. Okamoto, Y. Otomaru, K. Ueyama and T. Hayashi, *J. Am. Chem. Soc.*, 2005, **127**, 54–55; (e) E. Oblinger and J. Montgomery, *J. Am. Chem. Soc.*, 1997, **119**, 9065–9066.
- 7 (a) R. A. Fernandes, A. K. Jha and P. Kumar, *Catal. Sci. Technol.*, 2020, **10**, 7448–7470; (b) J. Takacs and X.-t. Jiang, *Curr. Org. Chem.*, 2003, **7**, 369–396; (c) D. H. Camacho, S. Saito and Y. Yamamoto, *Tetrahedron Lett.*, 2002, **43**, 1085–1088; (d) L. S. Hegedus, in *Comprehensive Organic Synthesis*, ed. B. M. Trost and I. Fleming, Pergamon: Oxford, 1990, vol. 1994, p. 1571.
- 8 (a) G. Frenking and N. Frohlich, *Chem. Rev.*, 2000, **100**, 717–774; (b) J. Chatt and L. A. Duncanson, *J. Chem. Soc.*, 1953, 2939–2947.
- 9 B. K. Liebov and W. D. Harman, *Chem. Rev.*, 2017, **117**, 13721–13755.
- 10 (a) X. Yan, X. M. Yang, P. Yan, B. Zhao, R. Zeng, B. Pan, Y. C. Chen, L. Zhu and Q. Ouyang, *Chem. Sci.*, 2023, **14**, 4597–4604; (b) S. Z. Tan, P. Chen, L. Zhu, M. Q. Gan, Q. Ouyang, W. Du and Y. C. Chen, *J. Am. Chem. Soc.*, 2022, **144**, 22689–22697; (c) X. X. Yang, R. J. Yan, G. Y. Ran, C. Chen, J. F. Yue, X. Yan, Q. Ouyang, W. Du and Y. C. Chen, *Angew. Chem., Int. Ed.*, 2021, **60**, 26762–26768; (d) B. X. Xiao, B. Jiang, R. J. Yan, J. X. Zhu, K. Xie, X. Y. Gao, Q. Ouyang, W. Du and Y. C. Chen, *J. Am. Chem. Soc.*, 2021, **143**, 4809–4816.
- 11 (a) Z. Wang, J. Wu, W. Lamine, B. Li, J. M. Sotiropoulos, A. Chrostowska, K. Miqueu and S. Y. Liu, *Angew. Chem., Int. Ed.*, 2021, **60**, 21231–21236; (b) Q. He, L. Zhu, Z. H. Yang, B. Zhu, Q. Ouyang, W. Du and Y. C. Chen, *J. Am. Chem. Soc.*, 2021, **143**, 17989–17994; (c) Y. Yang, J. Jiang, H. Yu and J. Shi, *Chem.–Eur. J.*, 2018, **24**, 178–186; (d) S. Xu, Y. Zhang, B. Li and S. Y. Liu, *J. Am. Chem. Soc.*, 2016, **138**, 14566–14569.
- 12 M. J. Frisch, *et al.*, Gaussian 09, Gaussian Inc., Wallingford, CT, 2013.
- 13 (a) A. D. Becke, *J. Chem. Phys.*, 1993, **98**, 5648–5652; (b) A. D. Becke, *Phys. Rev. A*, 1988, **38**, 3098–3100.
- 14 Y. Zhao and D. G. Truhlar, *Theor. Chem. Acc.*, 2007, **120**, 215–241.
- 15 A. V. Marenich, C. J. Cramer and D. G. Truhlar, *J. Phys. Chem. B*, 2009, **113**, 6378–6396.
- 16 (a) Z. Wang, Y. Zhou, W. H. Lam and Z. Y. Lin, *Organometallics*, 2017, **36**, 2354–2363; (b) T. Fan, K. S. Fu and Z. Lin, *Organometallics*, 2013, **32**, 5224–5230; (c) F. Schoenebeck and K. N. Houk, *J. Am. Chem. Soc.*, 2010, **132**, 2496–2497; (d) V. S. Bryantsev, M. S. Diallo and W. A. Goddard III, *J. Phys. Chem. B*, 2008, **112**, 9709–9719; (e) C. P. Kelly, C. J. Cramer and D. G. Truhlar, *J. Chem. Theory Comput.*, 2005, **1**, 1133–1152.
- 17 C. Y. Legault CYLview, 1.0b, Université de Sherbrooke, Sherbrooke, Canada, 2009, <http://www.cylview.org>.
- 18 To distinguish the role of Lewis acid or base in the metal-alkyne complex, the electron density of typical Lewis acid metal-alkyne complexes was considered. Calculated results indicate a significant charge transfer from alkyne to metal in the Pd(II) or Au(I) complexes, which is against the Lewis base mode in the (Ph<sub>3</sub>)P<sub>2</sub>Pd(0)–alkynal complex. Please see ESI† for more details.
- 19 (a) K. Zhong, S. Liu, X. He, H. Ni, W. Lai, W. Gong, C. Shan, Z. Zhao, Y. Lan and R. Bai, *Chin. Chem. Lett.*, 2023, **34**, 108339; (b) M. Liu, J. Sun and K. M. Engle, *Tetrahedron*, 2022, **103**, 132513.
- 20 (a) M. A. Ortuño, A. Lledós, F. Maseras and G. Ujaque, *ChemCatChem*, 2014, **6**, 3132–3138; (b) B. P. Carrow and J. F. Hartwig, *J. Am. Chem. Soc.*, 2011, **133**, 2116–2119; (c) C. Amatore, A. Jutand and G. Le Duc, *Chem.–Eur. J.*, 2011, **17**, 2492–2503.
- 21 (a) C. Joshi, J. M. Macharia, J. A. Izzo, V. Wambua, S. Kim, J. S. Hirschi and M. J. Vetticatt, *ACS Catal.*, 2022, **12**, 2959–2966; (b) Y. Wang, X. Qi, Q. Ma, P. Liu and G. C. Tsui, *ACS Catal.*, 2021, **11**, 4799–4809.
- 22 (a) P. Steinhoff and M. E. Tauchert, *Beilstein J. Org. Chem.*, 2016, **12**, 1573–1576; (b) M. Yamashita, I. Takamiya, K. Jin and K. Nozaki, *Organometallics*, 2006, **25**, 4588–4595; (c) K. Tatsumi, R. Hoffmann, A. Yamamoto and J. K. Stille, *Bull. Chem. Soc. Jpn.*, 1981, **54**, 1857–1867.
- 23 It's worth noting that both **3a** and **4a** were detected with a ratio of close to 1:1.6 in the presence of PCy<sub>3</sub>. While only **3a** was detected in the presence of PPh<sub>3</sub>.

